On-line temperature measurement during power cycle of PCB-embedded diode

Said Bensebaa, Mounira Bouarroudj-Berkani, Mickael Petit, Stéphane Lefebvre

Version of Record: https://www.sciencedirect.com/science/article/pii/S0026271421002791
Manuscript_ccdc51a3e6d226e5594521f205cf5af6

On-line temperature measurement during power cycle of PCB-embedded diode

S. BENSEBAA[a], M. BERKANI[b], M. PETIT[a], S. LEFEBVRE [a]

[a] *SATIE, École normale supérieure Paris-Saclay, CNRS, UCP, Cnam, France.*
[b] *SATIE, Université Paris Est Créteil UPEC, France*

Abstract

This paper presents an original methodology and a test bench for active power cycling and on-line junction temperature measurement during power cycling of power devices embedded in PCB. This method is based on the use of the ratio between forward voltage and forward current variations (ΔV_F, ΔI_F) during conduction period to estimate the thermal voltage U_T and thus the junction temperature in real time. The objective of this study is to estimate the junction temperature even for high frequency of power cycling tests. First, the measurement method is presented, and then the test bench is described.

1. Introduction

Power cycling test is one of the major methods used to study the reliability performance and evaluate lifetime of power converters with respect to the temperature stresses. In classical power cycling methods, the junction temperature measurement is performed using thermal sensitive electrical parameters (TSEP), such as on-state voltage at low current (for bipolar components : IGBTs and diodes…) [1] or threshold voltage V_{th} for MOSFET [2]. These methods are complicated to implement when power cycling is done under electrical constraints of the PWM type. A precise calibration is also necessary for each component before testing. This paper presents an innovative test bench for on-line junction temperature measurement during power cycling in order to study the reliability of power diodes embedded in PCB [3]. The proposed method is based on the use of the forward voltage V_F and forward current I_F variations during conduction period to estimate the thermal voltage U_T and thus the junction temperature in real time. This helps to get a good approximation even for high cycling frequencies (> 1 kHz). Table.1 gives a brief comparison between classical methods and the proposed one. First, a description of the method is given, and then a representative design of the power cycling circuit is presented.

2. Test bench

2.1. General description of the test bench

Fig. 1 describes the operating mode of the proposed test bench. A digital signal processor DSP (LAUNCHXL-F28379D) is used in this study to generate the control signals for the test bench but also to insure the acquisition of the voltage and current on the Device Under Test (DUT) by its internal ADC (Analog-to-digital converter). The DSP is connected to Matlab/Simulink® software via USB connection in order to transfer the operating code and ageing conditions (maximum junction temperature T_{Jmax}, ΔT_J, duration of the heating and cooling phases, nominal current $I_{N,}$...). According to these ageing conditions and measurements collected form ADCs inputs, the DSP generates the appropriate PWM output signals to control switches of the power circuit for heating or cooling the DUT.

2.2. Description of the junction temperature measurement method

This method consists of using the forward voltage V_F and forward current I_F evolutions during diode conduction. In fact, the current injected in the DUT during the ageing process must have ΔI_F ripples around an average current I_{F_AVG}. This current generates a voltage variation ΔV_F on the diode. By using these variations (ΔV_F and ΔI_F) the junction temperature can be estimated.

Table. 1. Comparison of different methods criteria for thermal junction temperature measurement [4].

Method	Voltage measurement with a low current injection	V_{th} with low current	The Proposed method
description	Sourcing a low current under on-state.	Sourcing a low current to the DUT with the gate-drain/collector in short-circuit.	Using the forward voltage V_F and forward current I_F variations
On/off line	Off-line	Off-line	On-line
Power device	IGBT /Diode	MOSFET	Diode/ (IGBTs in future)
Physical Quantities to be measured	Voltage drop measurement	Vgs voltage measurement	Measuring ΔI_F and ΔV_F variations to estimate thermal voltage U_T

* Corresponding author. said.bensebaa@satie.ens-cachan.fr
Tel: +33 (06) 60112495

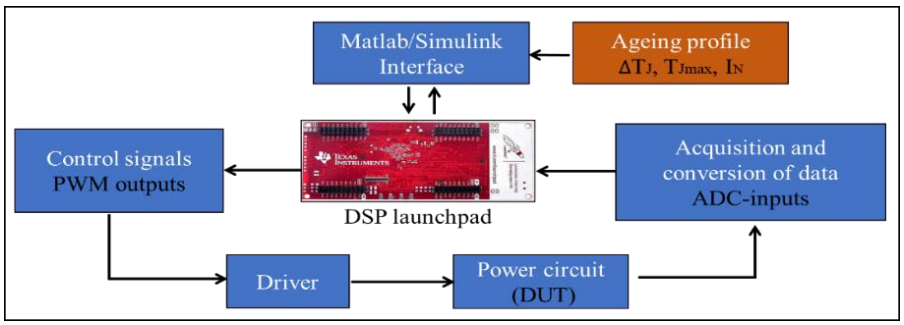

Fig. 1. The operating schematic of the proposed test bench.

The current-voltage function $I_F = f(V_j)$ of an ideal diode (general Shockley ideal diode equation) is given by equation (1), and is indicated by the blue curve in Fig. 2.

$$V_j = \eta . U_T . ln(1 + \frac{I_F}{I_s}) \quad (1)$$

Where V_j is the junction voltage, U_T is the thermal voltage, η the emission coefficient and I_s the reverse biased saturation current. U_T depends linearly on the junction temperature T_j by the equation (2).

$$U_T = \frac{k.T_j}{q} \quad (2)$$

Where k and q are the Boltzmann constant, and electron charge respectively.

The black curve in Fig. 2 shoes the forward characteristic $I_F = f(V_F)$ of the diode under test DUT. The relationship between the forward voltage V_F and forward current I_F for the considered packaging is given by equation (3).

$$V_F(I_F) = V_j + R_P . I_F \quad (3)$$

Where R_P represents the package resistance, in our case (for an embedded power diode in PCB [3]) it represents the metal foam resistance and contact resistances.

By calculating the slope of the $I_F = f(V_F)$ curve for a fixed average current, the sum of the package resistance R_P and the internal diode resistance r_D (related to Shockley diode model) are obtained, this resistance is named R_{total} and is given by equation (4).

$$\frac{\Delta V_F}{\Delta I_F} = \frac{\Delta(V_j + R_P . I_F)}{\Delta I_F} = \frac{\Delta V_j}{\Delta I_F} + R_P = r_D + R_P = R_{total} \quad (4)$$

By subtracting the product $(R_{total} \cdot I_F)$ from the forward voltage V_F, the red voltage curve is obtained, see equation (5). This latter is shifted by the product of $(r_D \cdot I_F)$ in comparison to the junction voltage V_j, see Fig. 2.

$$V_j(shifted) = V_F - (R_P + r_D) . I_F \quad (5)$$

To reach the thermal voltage U_T (so the junction temperature T_j) during the conduction period of the DUT, it is necessary to evaluate the ratio $\Delta V_j / \Delta I_F$ (which represents r_D), and for this purpose, the following steps are required:

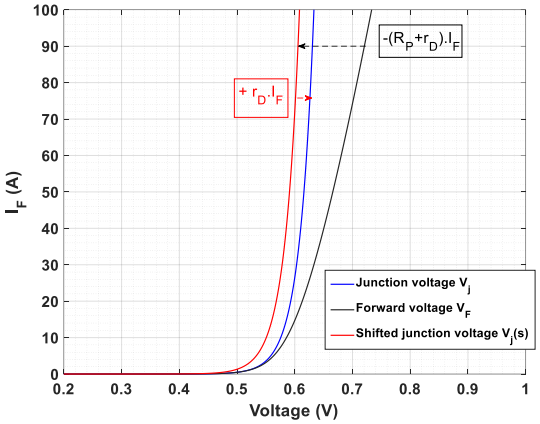

Fig. 2. Forward characteristics $I_F = f(V_F)$ of an embedded power diode (black curve); the $I_F = f(V_j)$ function of an ideal Shockley diode model (blue curve).

The first step consists of injecting a triangular current I_{F1} in the DUT with an average current I_{F1_AVG} and a current ripple ΔI_{F1}. The corresponding measured voltage across the DUT is V_{F1} with average voltage V_{F1_AVG} and a voltage ripple ΔV_{F1}, as illustrated on Fig. 3. With the use of ΔV_{F1} and ΔI_{F1} the resistance (R_{total}) is achieved using equation (4), and the junction voltage V_{01_AVG} is obtained from equation (6).

$$V_{01\_AVG} = V_{F1\_AVG} - (R_{total}) . I_{F1\_AVG} \quad (6)$$

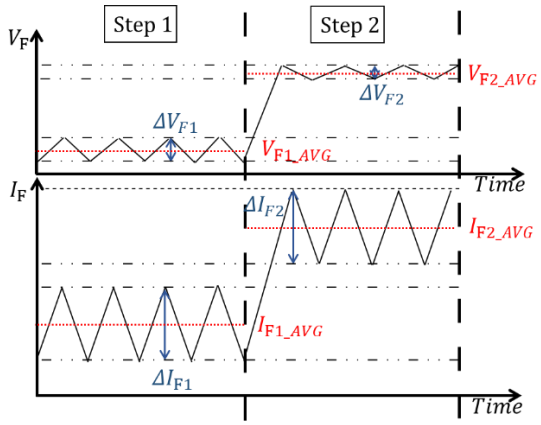

Fig. 3. Different steps for junction temperature estimation of the proposed method.

The second step consists of injecting a triangular current I_{F2} with a higher average current value $I_{F2\_AVG} > I_{F1\_AVG}$, as illustrated in Fig. 3. This allows to generate ΔI_{F_AVG} variations $(I_{F2\_AVG} -$

I_{F1_AVG}) and to achieve the ratio $\Delta V_j/\Delta I_F$, Fig. 4. Similarly, the new junction voltage V_{02_AVG} is given by equation (7).

$$V_{02\_AVG} = V_{F2\_AVG} - (R_{total}).I_{F2\_AVG} \quad (7)$$

According to equation (1) the junction voltage V_j depends on the forward current I_F and the saturation current I_S. If we calculate the derivative of V_j with respect to I_F, we obtain the value of the thermal potential U_T, as shown in equations (8-9).

$$\frac{\partial V_j}{\partial I_{F\_AVG}} = \frac{\partial(U_T.\eta.ln(1+\frac{I_F}{I_s}))}{\partial I_{F\_AVG}} \quad (8)$$

$$\frac{\partial V_j}{\partial I_F} = \frac{\eta.U_T}{I_s}.\frac{1}{(1+\frac{I_F}{I_s})} \quad (9)$$

Saturation current I_s is neglected in comparison to forward current I_F (I_s in the range of pA), so to get a better junction temperature approximation, the measurement must be done in the linear part of the forward characteristic $I_F = f(V_F)$. The obtained results are given in equations (10) and (11).

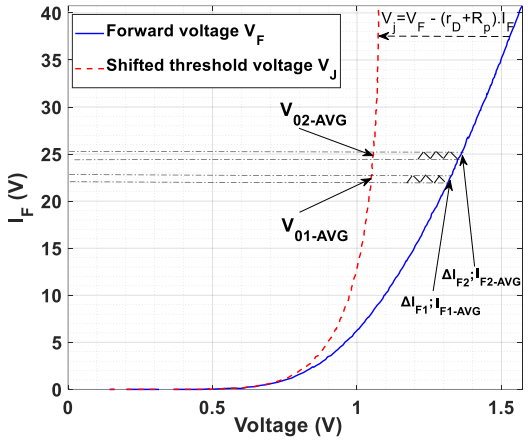

Fig. 4. Junction temperature estimation using the proposed method.

$$\frac{\partial V_j}{\partial I_F} = \frac{\eta.U_T}{I_{F\_AVG}} \quad (10)$$

$$\eta.U_T = \frac{(V_{02\_AVG} - V_{01\_AVG})}{(I_{F2\_AVG} - I_{F1\_AVG})} \cdot I_{F\_AVG} \quad (11)$$

Where I_{F_AVG} is equal to $(I_{F2\_AVG} + I_{F1\_AVG})/2$.

2.3. Method validation

The main goal is to apply this method on our PCB packaging, but as a first step, the feasibility of the proposed method was tested on a commercial Schottky diode (ref: PBYR3045PT).

As mentioned before, the presented method is based on using diode model given in equation 12. First, in order to verify if our diode model is valid for any temperature, the forward static characteristics $I_F = f(V_F)$ of the PBYR3045PT diode have been traced for different temperatures (10°C, 27°C, 47°C and 65°C), by using a thermal chamber and a Tektronix 371 Curve Tracer. For each temperature, 16 successive traces were performed and the mean one was plotted in Fig. 5.

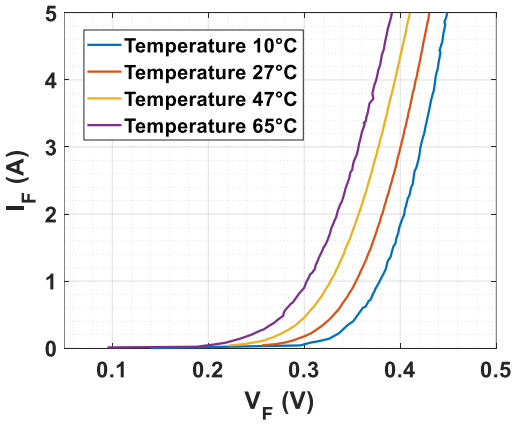

Fig. 5. Forward static characteristics $I_F = f(V_F)$ of a diode for different temperatures

Curves demonstrated in Fig. 5 have been fitted to data points, according to the equation presented in (12). Data calculated by the Matlab® curve fitting tool are $(\eta.U_T), I_s$ and R_P.

$$V_F = (\boldsymbol{\eta.U_T}).ln(1+\frac{I_F}{\boldsymbol{I_s}}) + \boldsymbol{R_P}.\ I_F \quad (12)$$

As it can be seen in Table.2, the goodness-of-fit parameter (R-square) is close to one for all temperatures, which means that curves are well-fitted. Moreover, it can be noticed that a perfect linearity between the thermal voltage and the temperature is obtained, even if a high current passes through the diode. These results are promising, and confirm that the model in equation 12 is working properly, thus, the proposed method can be used without any problem. The measurement sensitivity is in the range of 0,09 (mV/°C), therefore, our test bench must be able to measure voltages in the range of 1 µV.

Table. 2. Obtained results from the fitting curve tool.

Temperature T (°C)	***10°C***	***27°C***	***47°C***	***65°C***
I_S (µA)	0,566	3,247	18,05	73,81
R_P (mΩ)	7,257	8,07	8,855	9,624
$\eta.U_T$ (mV)	25,83	27,38	29,18	30,83
$\Delta(\eta\ U_T)\ /\ \Delta T$	In the range of 0,09 mV/°C			
Emission-coefficient η	1.0582	1.0582	1.0572	1.0575
R-square	0.9999	1	0.9999	1

2.3.1 Validation using a fitted diode model.

To verify the possibility of reaching the appropriate thermal potential for a given temperature (e.g. 27°C) by the proposed method, the $I_F = f(V_F)$ forward characteristics were traced for a temperature of 27°C, according to the extracted parameters $(\eta.U_T), I_s$ and R_P (see Table.2). It is worth mentioning that it was possible to apply the method on the curve of the Fig.5 at 27°C, however, to avoid noises and to achieve accurate results the obtained curve from Table.2 parameters was preferred. Then by applying the different steps of the method (from equation 4 to 11) all along the current range of the diode (repeated each 50 mA along the $I_F = f(V_F)$ fitted trace with a step of ΔI_F=50 mA) the thermal

potential is obtained and results are depicted in Fig.6.

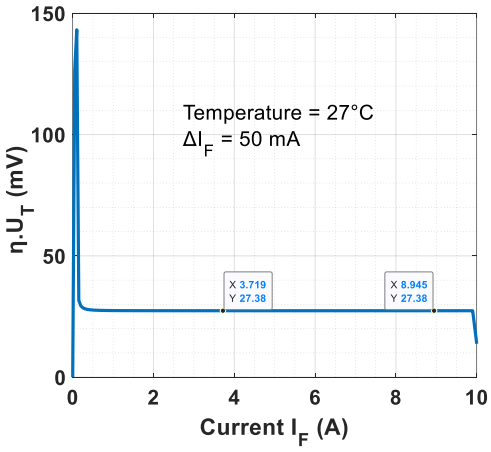

Fig. 6. Obtained thermal potential $(\eta.U_T)$ from $I_F = f(V_F)$ fitted trace in function of the injected current, at a temperature of 27°C.

Presented results in Fig.6 show that the obtained value of the product $(\eta.U_T)$ is 27,38 mV, which corresponds to the temperature of 27°C. The same value is obtained whatever the level of the applied average current, including the non-linear zone of the static characteristic $I_F = f(V_F)$. Therefore, the average applied current value has no effect on the estimation of the junction temperature.

Fig.7 shows the evolution of the different resistances as a function of the applied current. These resistances were deduced during thermal potential calculation (deduced each step of 50 mA). As illustrated in Fig.7, the Schottky diode internal resistance r_D decreases by the increase of the applied current, moreover, the package resistance R_P remains fixed whatever the value of the current (as it was expected).

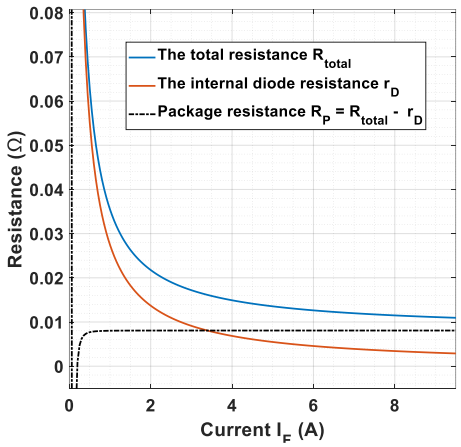

Fig. 7. Evolution of the calculated resistances in function of the applied current I_F at temperature of 27°C; the total resistance (blue), the internal resistance (red) and the difference between total and internal resistances (dotted line).

2.3.2 Validation using an experimental test.

In order to validate the obtained results, an experimental test was performed in order to verify if the same appropriate thermal potential could be reached when injecting current pulses on the diode. For this purpose, a Schottky diode was mounted on a cooler and then was inserted in a thermal conditioner (to impose a constant temperature of 27°C). Then, current pulses were injected (from 0 to 10 A, with a step of 50 mA) on diode terminals through a power supply (RSPS-6-200). These pulses are repeated each 7 seconds with an on-state duration of 1 second. The choice of a low frequency pulse repetition helps to avoid the accumulation of heat on the cooler between two successive pulses, Fig. 8.

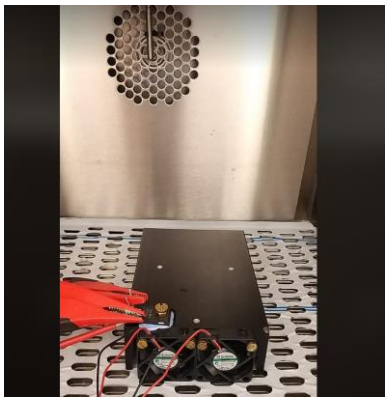

Fig. 8. Junction temperature measurement set up; the diode is mounted on a cooler via a thermal paste and is inserted inside a thermal conditioner.

Two digital multimeters (DDM 34461a) were used to measure the voltage and current across the diode. These multimeters have a feature of carrying out an analog to digital conversion (ADC) with 32 bits. Thus, allowing to obtain a high-accuracy and high-precision measurements (in the range of µV). The accuracy of these multimeters depends on the period during which the ADC is reading the input signal. Therefore, to get the desired precision with this equipment, the acquisition time was set to 100 ms per sample. The different steps of the proposed method were applied on the measurements (obtained from digital multimeters). Results are depicted in Fig. 9 and show that for low currents the product $(\eta.U_T)$ is around 27 mV, and the higher the current level is applied the more noise is observed.

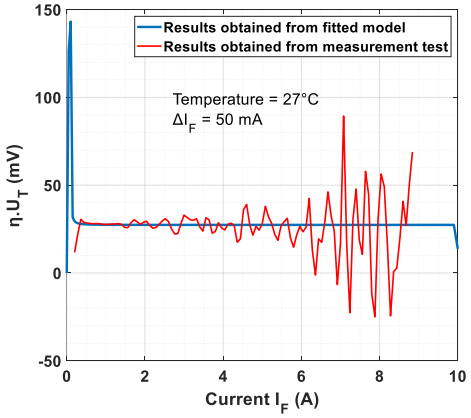

Fig. 9. Comparison between thermal potential $(\eta.U_T)$ obtained from $I_F = f(V_F)$ fitted trace (blue), and the one obtained from measurement test (red), at a temperature 27°C.

To understand the source of the noise in the thermal potential measurements and to follow the junction temperature evolution within diode terminals, the diode thermal behaviour was simulated using ANSYS Twin Builder© (from Electromagnetic suite) software, [7]. By using Z_{th} curve (from PBYR3045PT datasheet), the thermal model is extracted and diode's Foster parameters (R_{th} and C_{th}) are identified, Fig. 10.

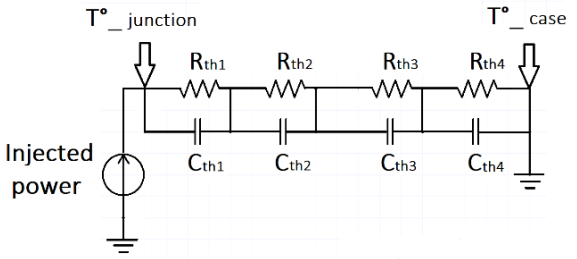

Fig. 10. Foster thermal model of the diode.

Once parameters identification is completed, the junction temperature evolution is observed when current pulses are injected within diode terminals (with the same configuration used before in the injected experimental current pulses). Obtained results are depicted in Fig. 11.

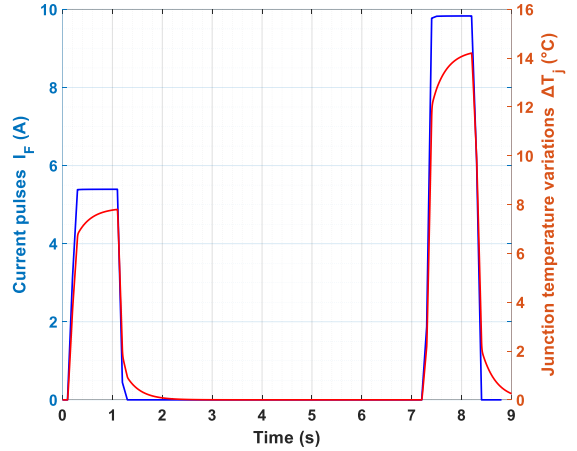

Fig. 11. Simulated junction temperature variations during the injection of current pulses, (obtained by using the diode Foster thermal model).

Simulation results in Fig.11 show that when the current pulses are injected the junction temperature of the diode varies with a fast dynamic (in the range of ms), this variation depends on the amplitude of the injected current. The more the level of injected current increases, the more the junction temperature increases. In our case, for a pulse of 10 A the junction temperature increases with 14°C. As the measuring device (digital multimeter) performs measurements each 100 ms (sampling time), the measured voltage is not correct and does not correspond to the initial temperature that existed before injecting pulse current ($V_F + \Delta V_F$ due to the junction temperature variations). This explains the noise that appeared during the experiment measurement in Fig.9. Consequently, to perform a measurement with acceptable level of noise, it is necessary to carry out a very precise measurements (µV) and to be able to recover the measurement in less than 1 ms. Finally, it is necessary that the injected current ripples should be low as possible, in order to avoid overheating the junction temperature.

2.4. Circuit design.

To generate a current with controlled ripples during aging test, a boost converter has been added. This latter allows creating the desired ripple thanks to its inductance and to the transistor switching and allows to control the forward current. The circuit is depicted on Fig. 12. Note that the boost output is directly related to the DC voltage source; therefore, its output voltage is always equal to the DC source. Two differential amplifiers are inserted, the first one allows to measure the voltage at the DUT terminals and the second one allows measuring the image of the forward current through a shunt resistor. The outputs of these two amplifiers are directly connected to the ADC inputs (Analog-to-digital converter).

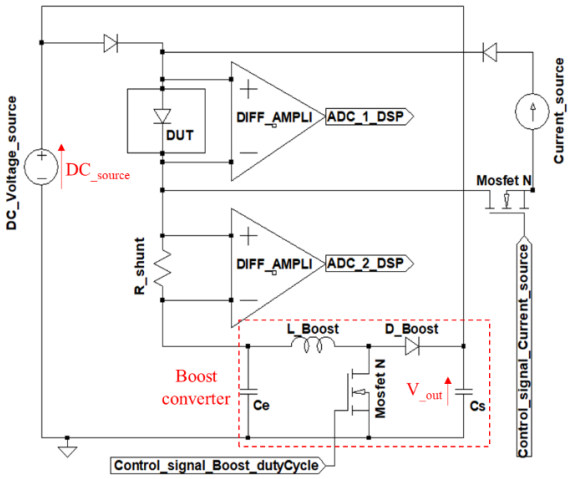

Fig. 12. The proposed schematic for power cycling.

A precise current source (a few mA) has been added in parallel to the terminals of the DUT. This allows estimating the junction temperature by the classical method (on-state voltage at low current) of TSEP measurement, during the power cycling cooling phase (where no power current crosses the DUT).

Fig. 13 shows the first prototype for power cycling test circuit with the DSP control part.

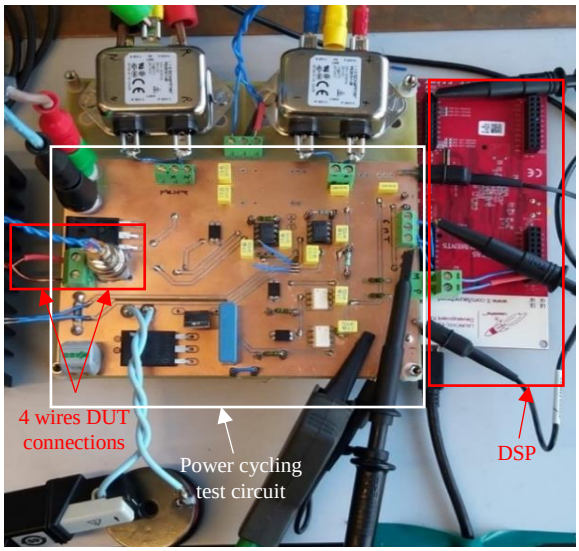

Fig. 13. First prototype of the power cycling test circuit, on the right DSP, on the left inputs for DUT connection.

The ADCs inputs on the DSP should be configured in such a way that they are triggered for acquisition at a precise time. For example, if we want to get the maximum forward current I_{F_max} the ADC should be triggered when the carrier signal is incrementing and equals to the modulating signal, see Fig. 14. Similarly, if we want to get the minimum forward current I_{F_min} the ADC should be triggered when carrier signal is decrementing and equals to modulating signal. Moreover, to get the average forward current I_{F_AVG} the ADC triggering is performed when carrier signal is equal to zero or period, see Fig. 14.

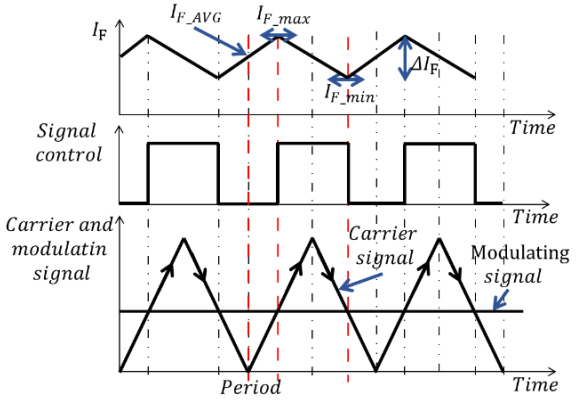

Fig. 14. Configuration of the ADCs triggering for acquiring the desired measurements points.

The next step is to find the appropriate equipment (ADC) which allows achieving a precise and accurate measurement with a very low acquisition time (less than 1 ms), in order to validate the test bench.

3. Conclusion

This paper presents a new methodology (and test bench) for on-line junction temperature measurement during power cycling of power diode packages. The measurement method is described and the test bench is presented. The results of the junction temperature measurement are promising; however, it is impossible to reach it without using a precise and accurate instrument with a very low acquisition time. The final objectives of this study (as future work) can be summarized as below.

- Apply the proposed method on our PCB packaging.
- Ageing several samples in parallel with the same DSP microcontroller, and with the possibility of having a different set points for each sample (ΔT_J, T_{Jmax} ...).
- To make an instantaneous regulation of the junction temperature, which allows having the same temperature in all samples even if they have different package resistances or even if the resistance changes during ageing test, [8].

References

[1] Y. Avenas, L. Dupont, and Z. Khatir, « Temperature Measurement of Power Semiconductor Devices by Thermo-Sensitive Electrical Parameters—A Review », IEEE Trans. Power Electron., vol. 27, no 6, p. 3081-3092, June 2012, doi: 10.1109/TPEL.2011.2178433.

[2] H. Chen, V. Pickert, D. J. Atkinson, and L. S. Pritchard, « On-line monitoring of the MOSFET device junction temperature by computation of the threshold voltage », in 3rd IET International Conference on Power Electronics, Machines and Drives (PEMD 2006), Dublin, Ireland, 2006, vol. 2006, p. 440-444, doi: 10.1049/cp:20060147.

[3] S. Bensebaa, M. Berkani, S. Lefebvre, M. Petit, N. Schmitt, and S. Zhang, « Reliability study of PCB-embedded power dies using solderless pressed metal foam », Microelectronics Reliability, vol. 114, p. 113904, nov. 2020, doi: 10.1016/j.microrel.2020.113904.

[4] L. Gopi Reddy, L. Tolbert, and B. Ozpineci, « Power Cycle Testing of Power Switches: A Literature Survey », IEEE Trans. Power Electron., p. 1-1, 2014, doi: 10.1109/TPEL.2014.2359015.

[5] N. Takashima and M. Kimura, « Diode temperature sensor with the output voltage proportional to the absolute temperature and its application to the thin film Pirani Vacuum Sensor », in IECON 2007 - 33rd Annual Conference of the IEEE Industrial Electronics Society, Taipei, nov. 2007, p. 2197-2202, doi: 10.1109/IECON.2007.4460257.

[6] J. Brandelero, J. Ewanchuk, and S. Mollov, « Online junction temperature measurements for power cycling power modules with high switching frequencies » , 28th International Symposium on Power Semiconductor Devices and ICs (ISPSD), June 12 – 16, 2016, Prague, Czech Republic, pp. 191-194.

[7] https://ansyshelp.ansys.com/account/secured?returnurl=/Views/Secured/prod_page.html?pn=ANSYS,%20Inc.%20Release%20Notes

[8] A. Stupar, D. Bortis, U. Drofenik, et J. W. Kolar, « Advanced setup for thermal cycling of power modules following definable junction temperature profiles », *in The 2010 International Power Electronics Conference - ECCE ASIA -*, Sapporo, Japan, June 2010, p. 962-969. doi: 10.1109/IPEC.2010.5542179.